SUPPLEMENTARY INFORMATION

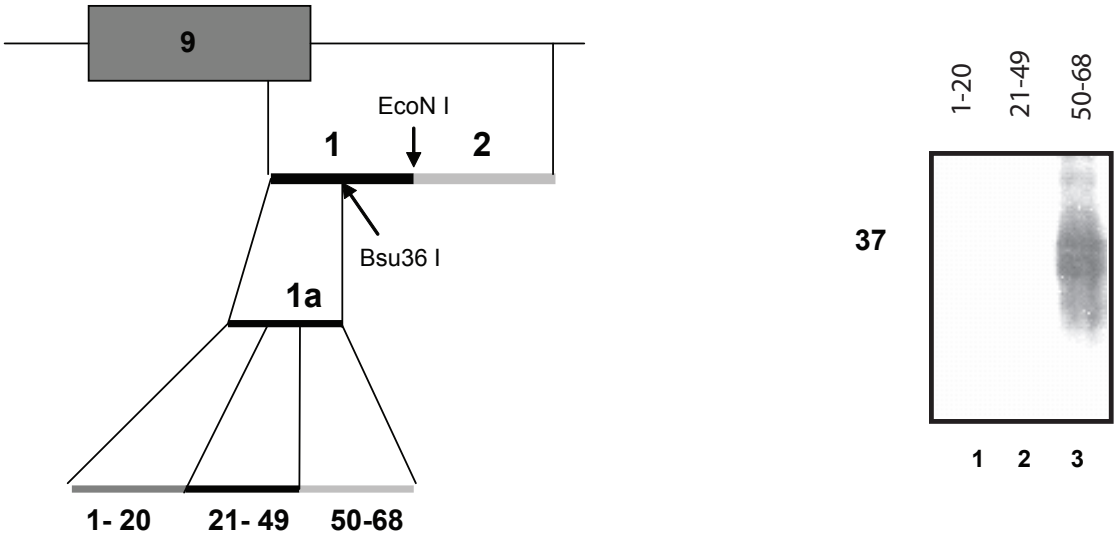

Supplementary Figure 1: Mapping of strong ~35-40 kDa crosslinking in the EI9 substrate. Truncations in EI9 were introduced with the indicated restriction enzymes (left). Strong crosslinking mapped to EI(1a) (not shown). Sections of EI9(1a) were cloned and used for UV crosslinking in HeLa NE.

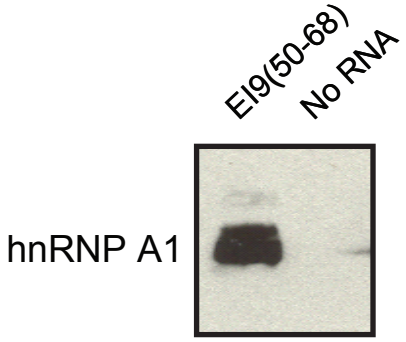

Supplementary Figure 2: hnRNP A1 binds to EI9(50-68). After RNA affinity chromatography using biotinylated EI9(50-68), protein samples from EI9(50-68) (lane 1) and no RNA control (lane 2) were separated on 10% SDS-PAGE and analyzed by immunoblotting using an anti-hnRNP A1 antibody.

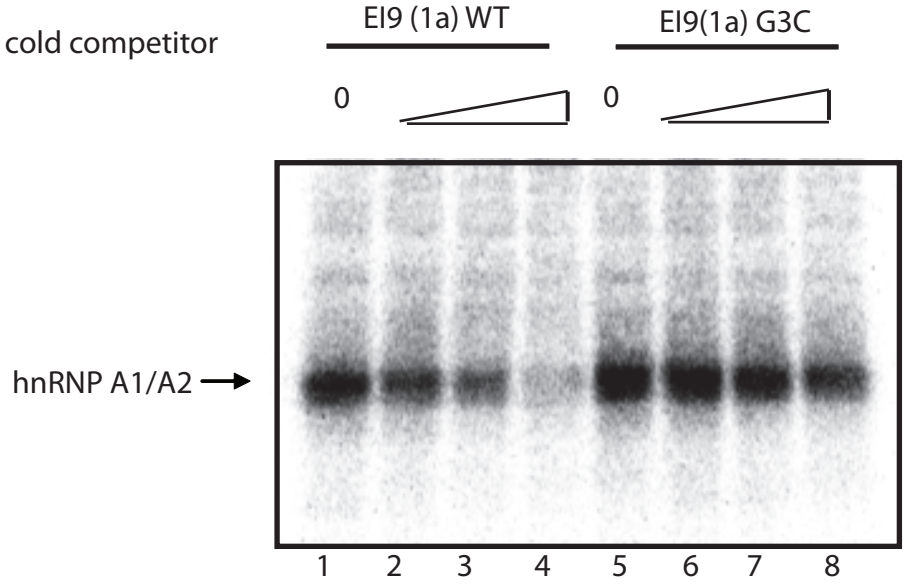

Supplementary Figure 3: hnRNP A1 binding to EI9(1a) is specifically decreased by G3C mutation. ^{32}P-UTP labeled EI9(1a) RNA (see diagram in Supplementary Figure 1) was incubated with HeLa NE, in the presence of increasing amount (0, 1.5, 3, 7.5 μM) of cold WT EI9(1a) RNA (lanes 1-4) or cold EI9(1a) G3C mutant RNA (lanes 5-8), followed by UV crosslinking..

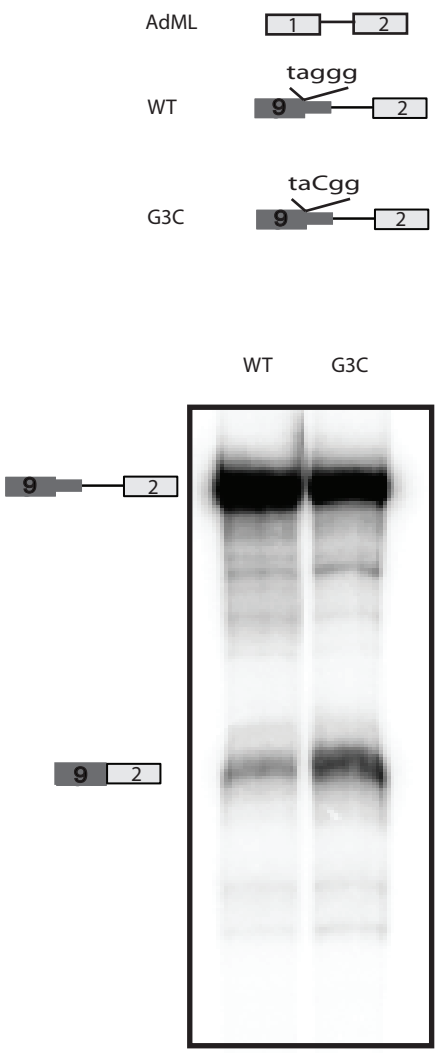

Supplementary Figure 4: Mutation of hnRNPA1/A2 binding site increases splicing of E9 containing in vitro splicing substrate. Schematic diagram of in vitro splicing constructs derived from AdML pre-mRNA substrate (top). In vitro splicing in HeLa nuclear extract using WT or G3C substrates.

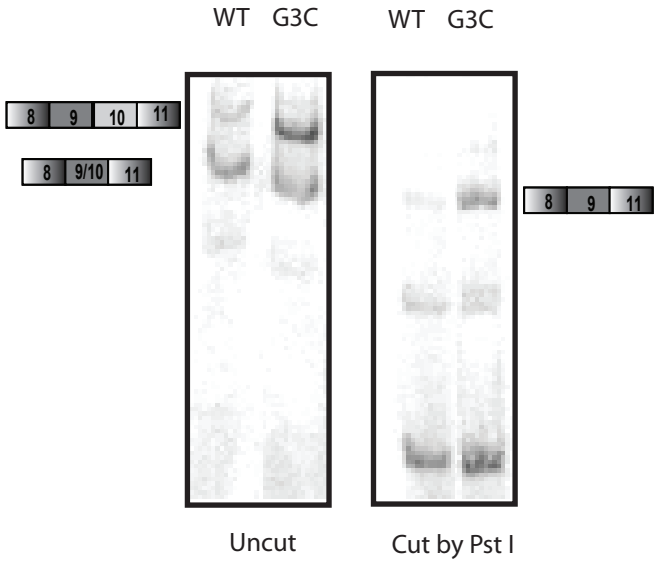

Supplementary Figure 5: Minigene with mutated hnRNPA1/A2 binding site increases inclusion of E9 in HeLa cells. The mutation results in an increase in E9 and E10 double inclusion (left panel). Single inclusion band at left G3C lane contains a higher proportion of E9 containing transcripts as determined by Pst I digestion (right panel).

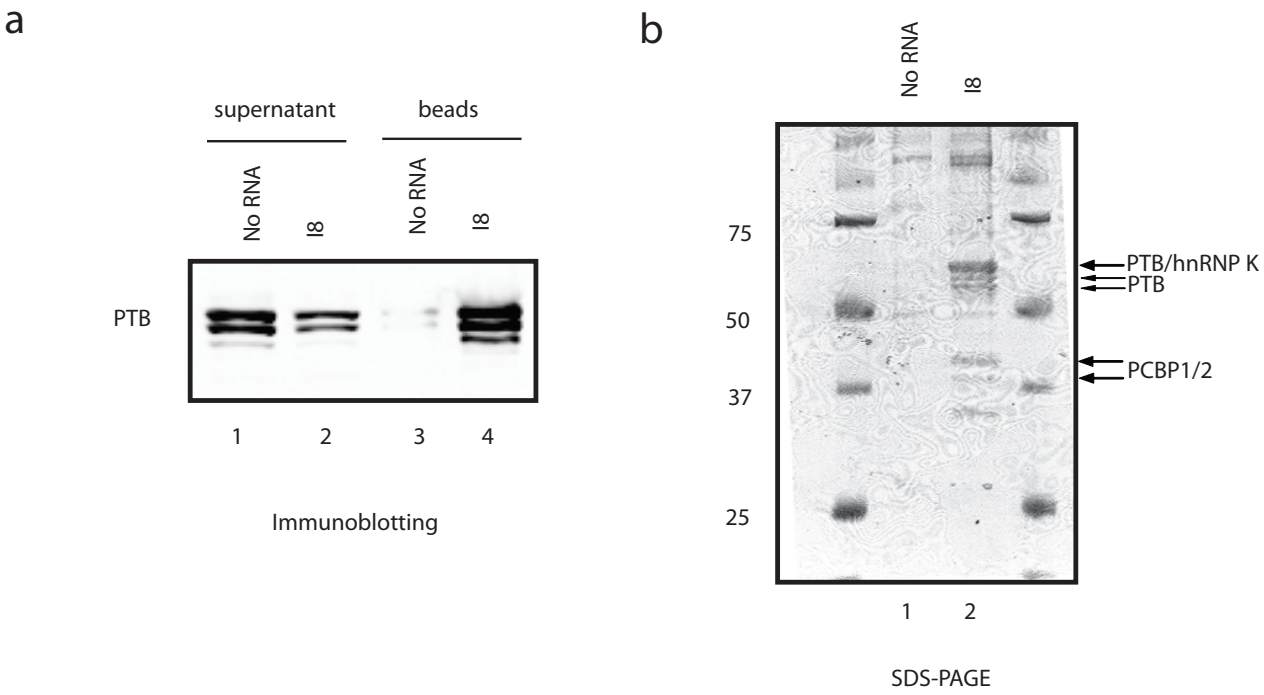

Supplementary Figure 6: a, PTB binds to biotinylated RNA oligo I8. After affinity chromatography using biotinylated I8 RNA supernatants (lanes 1 and 2) and protein samples bound to the beads from I8 (lane 4) and no RNA control (lane 3) were separated on 10% SDS-PAGE and analyzed by immunoblotting using an anti-PTB antibody (BB7). **b,** After RNA affinity chromatography using biotinylated I8, protein samples bound to the beads from I8 (lane 2) and no RNA control (lane 1) were separated on 10% SDS-PAGE and Coomassie stained. Positions of bands excised for mass spectrometry are indicated.

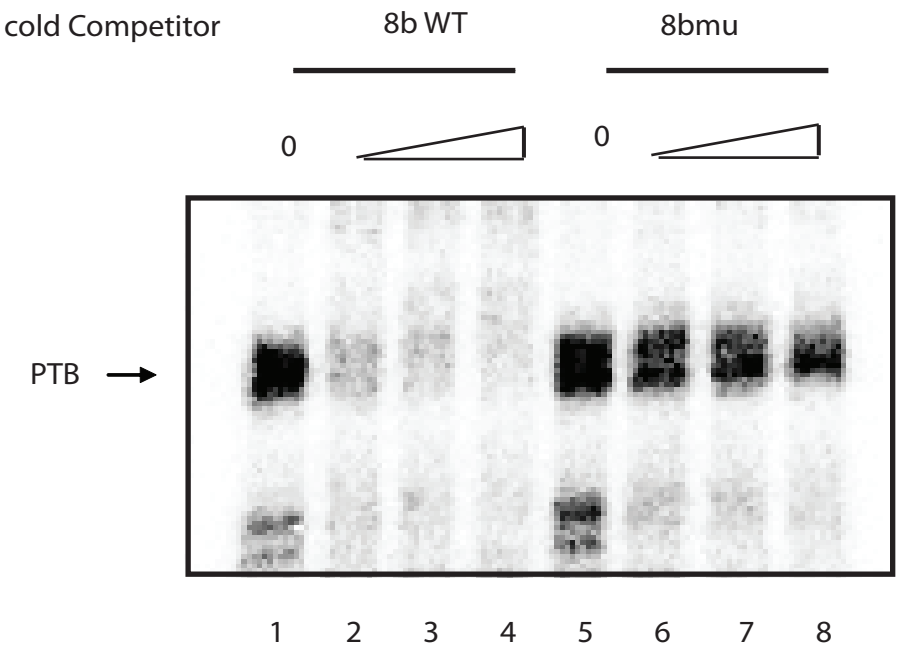

Supplementary Figure 7: PTB binding to I8 RNA is specifically abolished by a C to G mutation. ^{32}P -UTP labeled I8 RNA (see sequence in Fig. 1) was incubated with HeLa NE in the presence of increasing amounts (0, 2, 3,3 6 μM) of cold I8 WT RNA (lanes 1-4) or cold I8mu RNA (lanes 5-8), followed by UV crosslinking.

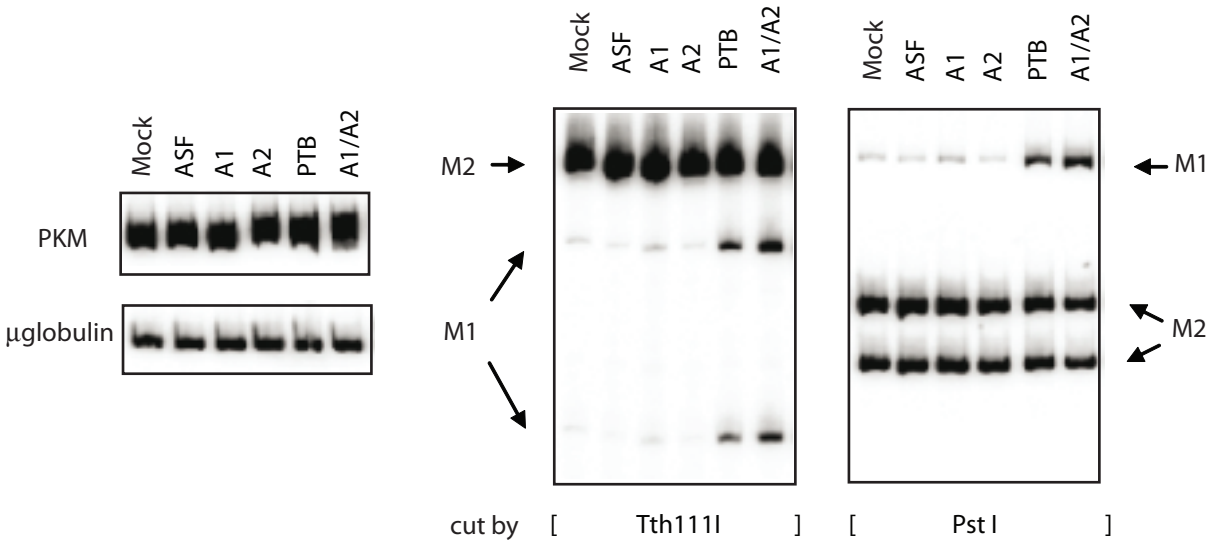

Supplementary Figure 8: Knockdowns of splicing factors have differing effects on PKM splicing. The indicated splicing factors were depleted by siRNA, followed by PKM splicing assay outlined in Fig. 1a. Products corresponding to M1 and M2 are indicated with arrows. PCR products for the PKM amplicon and a load control, µglobulin, are displayed at left. The PKM amplicons after cutting with the indicated enzyme are shown in the middle and right panels.

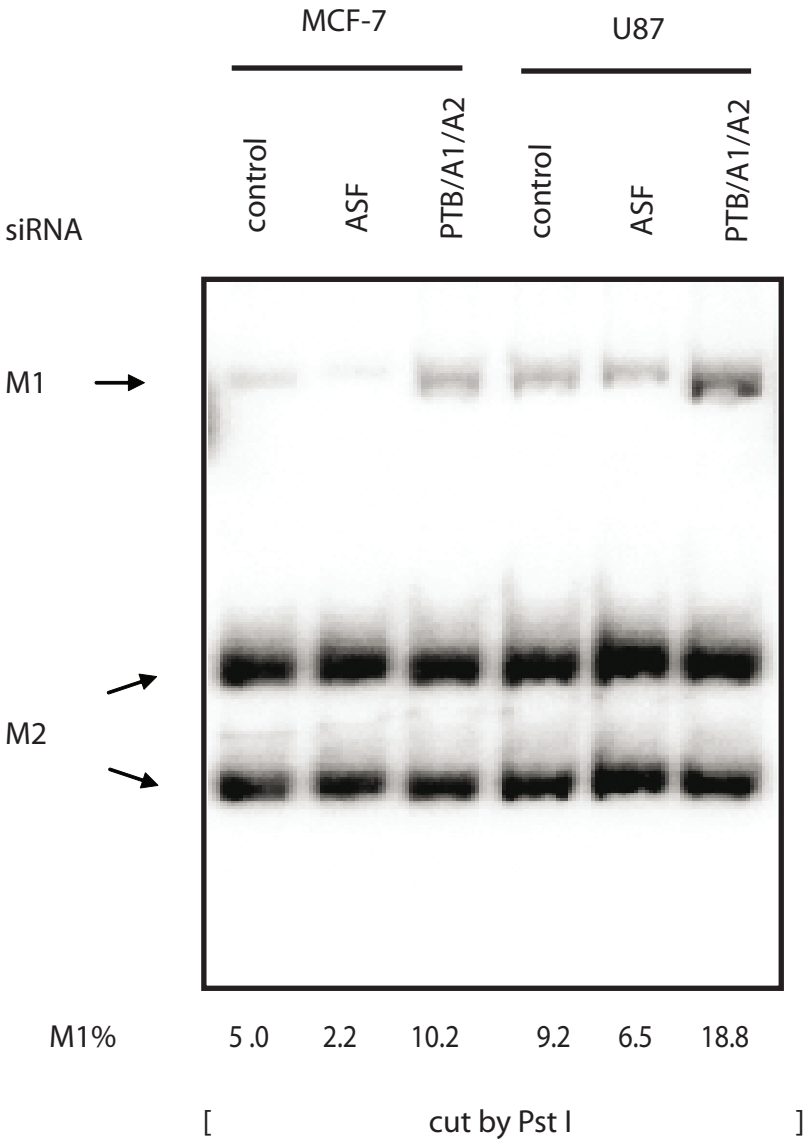

Supplementary Figure 9: Assay of PKM splicing after siRNA depletion of ASF/SF2, or simultaneous knockdown of PTB/A1/A2. siRNAs were transfected into human breast cancer cell line MCF-7 and glioblastoma cell line U87. Cells were collected after three days. Total RNA was extracted and PKM isoform ratio was estimated as described in Fig. 2a.

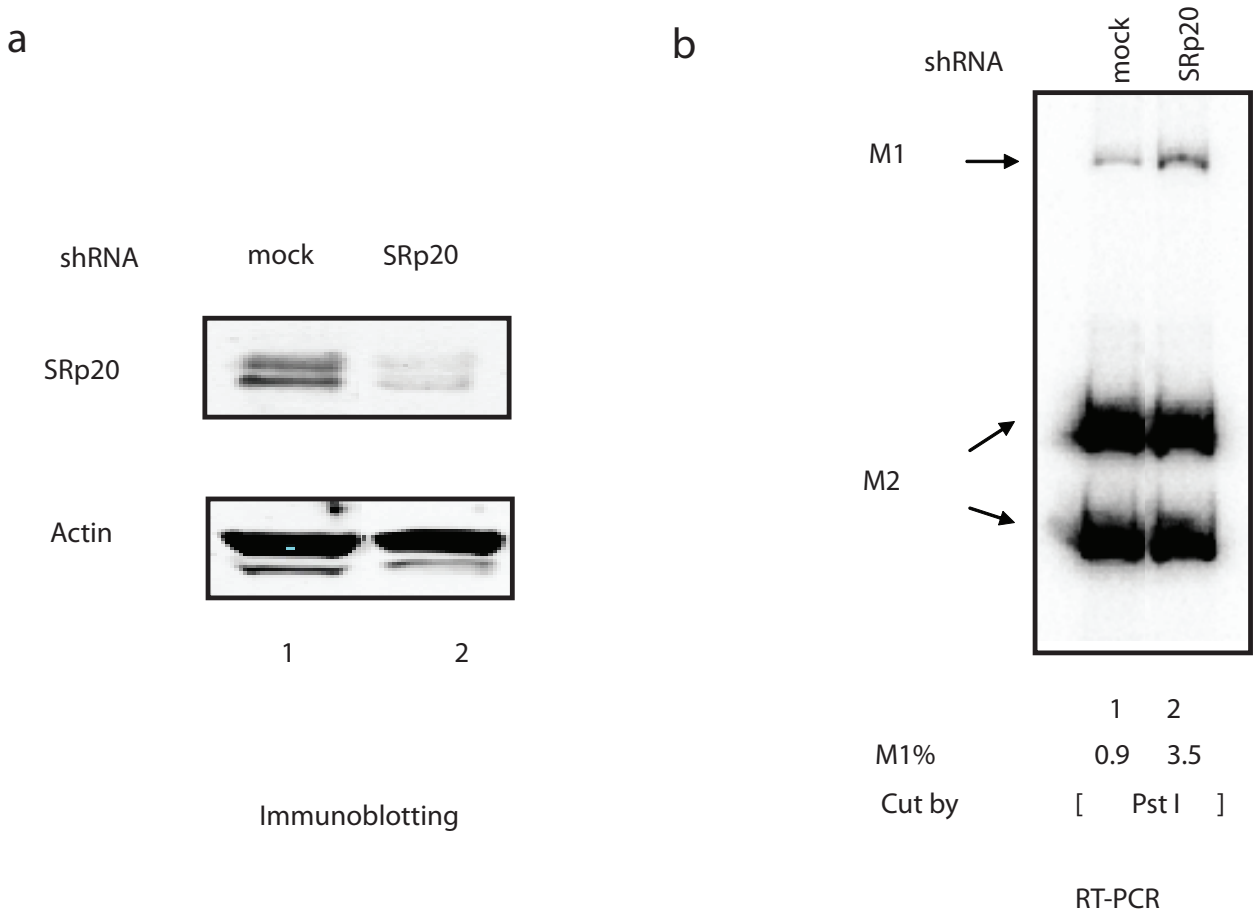

Supplementary Figure 10: SRp20 knockdown does not affect the PKM1/2 mRNA ratio. **a,** Immunoblotting to detect SRp20 protein levels in HeLa cells treated with either control shRNA (lane 1) or SRp20-targeting shRNA (lane 2). **b,** PKM1/2 ratios in control and SRp20 knockdown cells determined as in Fig. 2a.

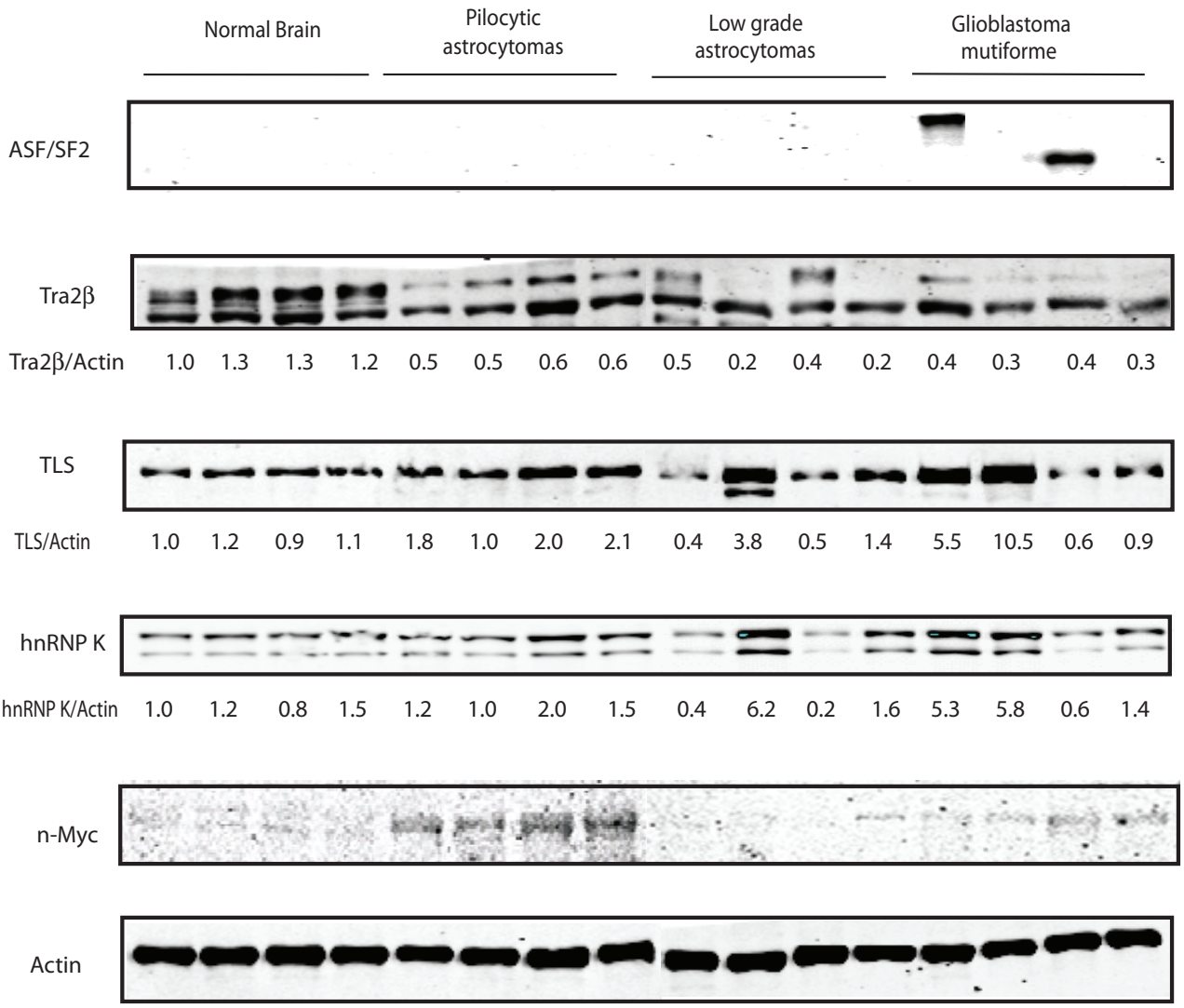

Supplementary Figure 11: Lysates of normal brain and glioma samples were immunoblotted for ASF/SF2, Tra2β, TLS, hnRNP K and n-Myc and normalized to actin. Quantitation of Tra2β, TLS and hnRNP K is indicated below each immunoblot (normal brain sample one=1). Sample order is the same as for RT-PCR and immunoblotting in Fig. 3c and 3d.

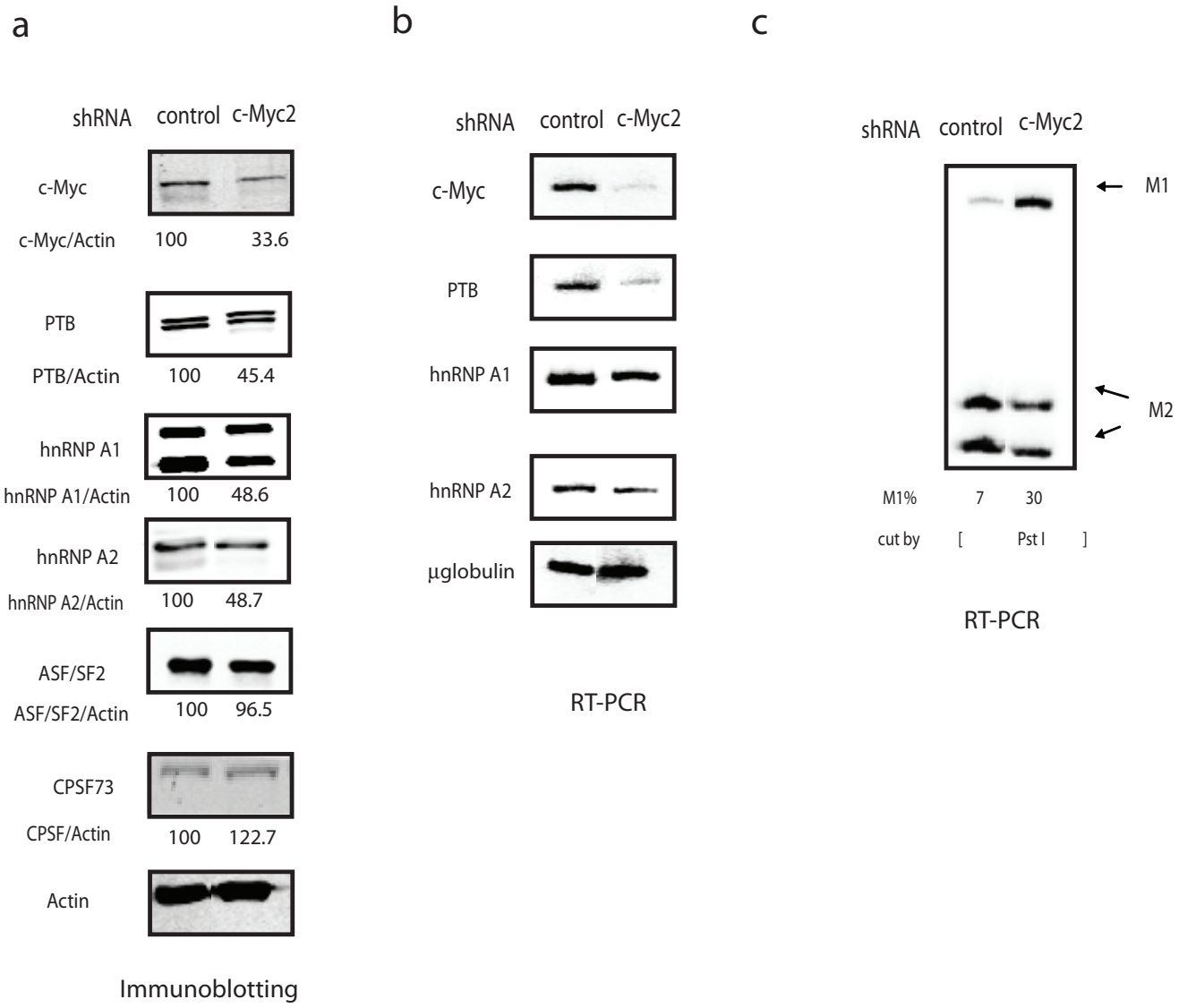

Supplementary Figure 12: A stable cell line expressing a second c-Myc-targeting shRNA also reduced PTB/A1/A2 and PKM2 mRNA levels. **a,** Immunoblotting using NIH-3T3 cells stably expressing control shRNA or c-Myc-targeting shRNA2. Signals were quantitated and normalized to actin. **b,** RT-PCR was used to determine relative mRNA levels in cells stably expressing control shRNA or c-Myc-targeting shRNA2. **c,** PKM1/2 ratios in control and c-Myc knockdown cells determined as in Fig. 2a.

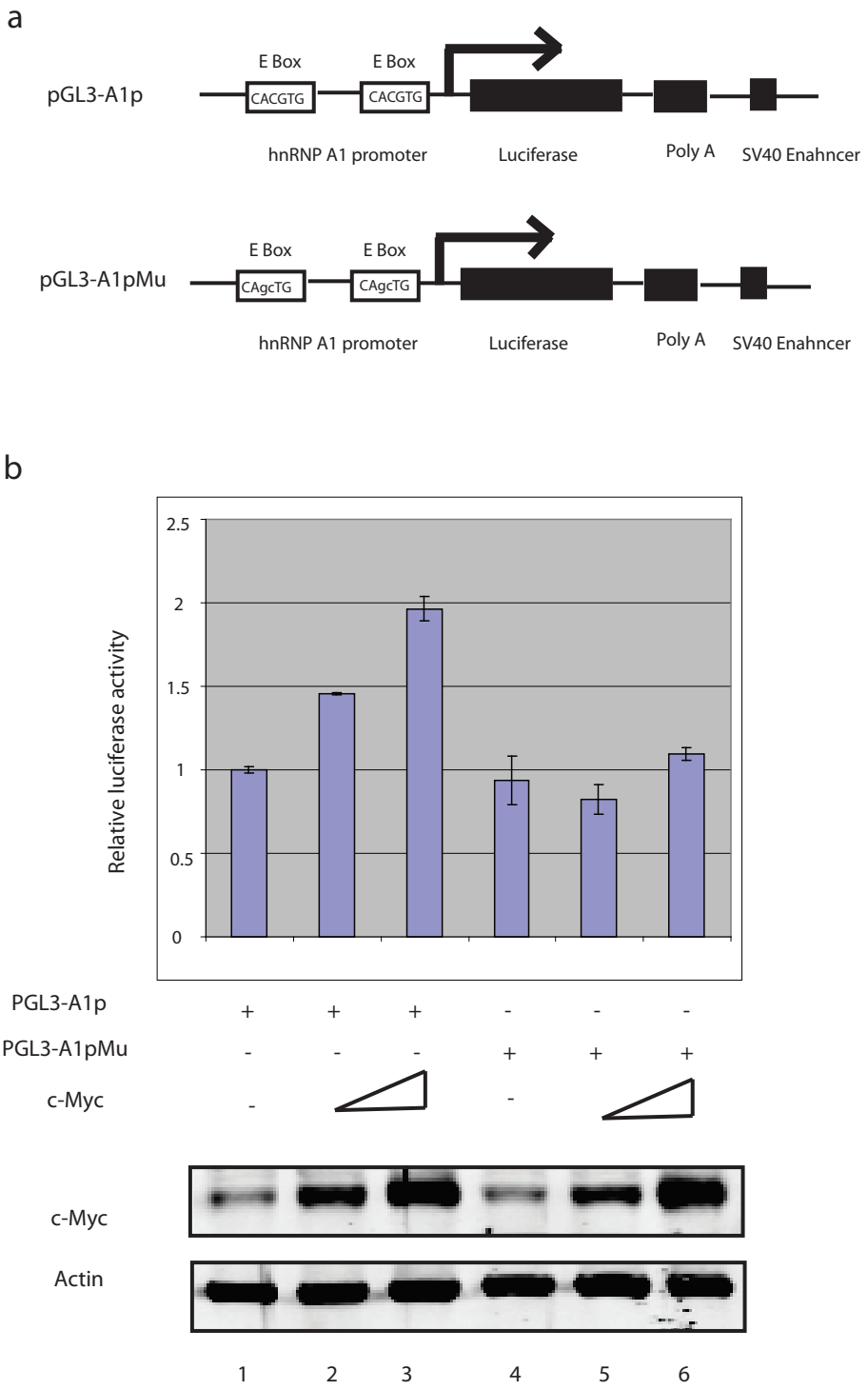

Supplementary Figure 13: c-Myc upregulates transcription from the hnRNP A1 promoter via E boxes. **a,** Diagrams showing hnRNP A1 promoter-Luciferase reporter constructs. E boxes (CACGTG) are putative c-Myc binding sites, which are located within a ~700 nt hnRNP A1 promoter region cloned upstream of the luciferase gene. pGL3-A1p contains the wild-type promoter region. pGL3-A1pMu contains mutated E boxes (indicated in the diagram). **b,** Results of dual luciferase reporter assays showing relative luciferase activity (top) activated by overexpression of c-Myc in HeLa cells by co-transfection of c-Myc expression vector and pGL3-A1p (lanes 1-3) or pGL3-A1pMu (lanes 4-6). Luciferase activity was normalized to Renilla luciferase activity, and pGL3-A1p activity was set as 1. Immunoblotting using c-Myc antibody to show c-Myc overexpression in transfected cells (bottom).

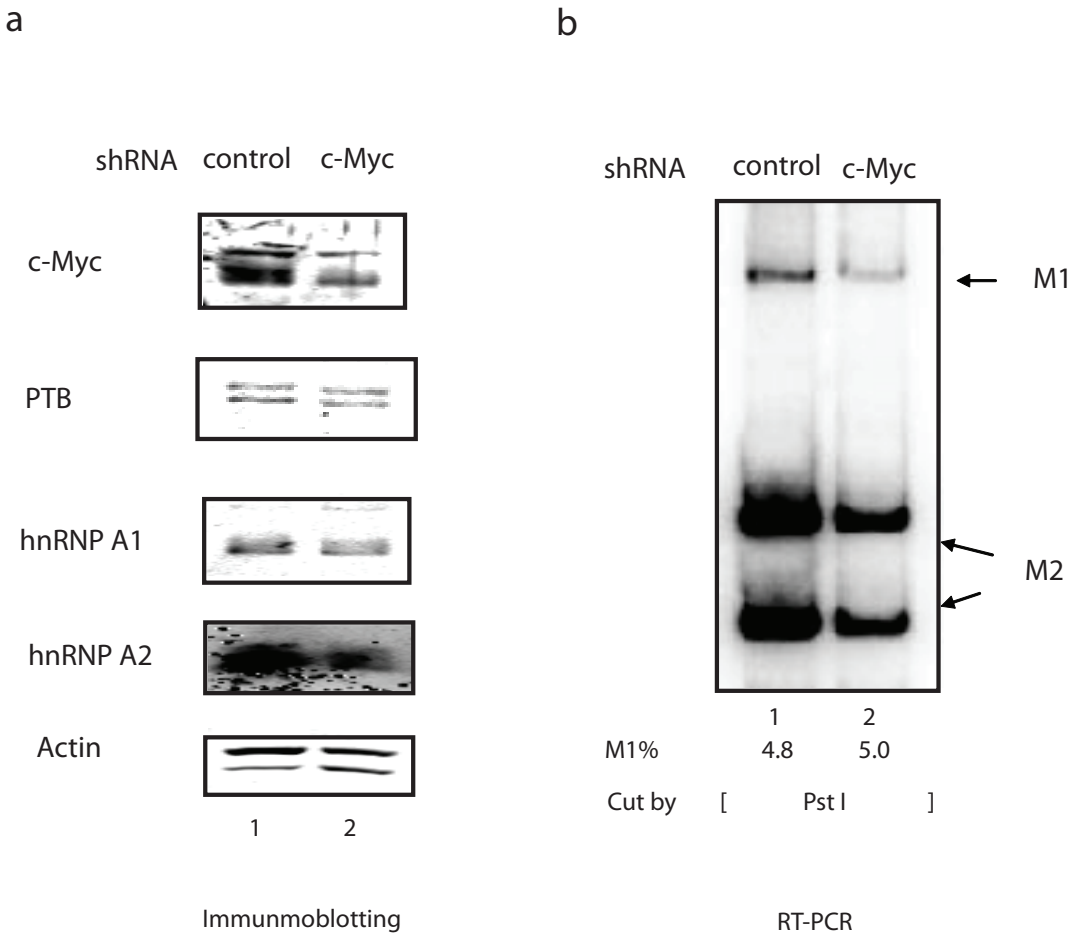

Supplementary Figure 14: c-Myc knockdown in HeLa cells does not change PKM splicing. **a,** Immunoblotting using HeLa cells transiently expressing control or human c-Myc-targeting shRNAs. **b,** PKM1/2 ratios in control and c-Myc knockdown cells determined as in Fig. 2a.